J|A|C|S ARTICLES

Published on Web 03/24/2010

Contiguous *O*-Galactosylation of 4(*R*)-Hydroxy-L-proline Residues Forms Very Stable Polyproline II Helices

Neil W. Owens, Jörg Stetefeld, Erika Lattová, and Frank Schweizer*

Department of Chemistry, University of Manitoba, Winnipeg, Manitoba R3T 2N2, Canada

Received July 10, 2009; E-mail: schweize@cc.umanitoba.ca

Abstract: The hydroxyproline-rich glycoproteins (HRGPs) are the major structural proteins of the extracellular matrix of algae and land plants. They are characterized by a rigid polyproline type II (PPII) conformation and extensive *O*-glycosylation of 4(*R*)-hydroxy-L-proline (Hyp) residues, which is a unique post-translational modification of proteins. The functional consequences of HRGP glycosylation remains unclear, but they have been implicated in contributing to their structural rigidity. Here, we have investigated the effects of naturally occurring β-*O*-galactosylation of Hyp residues on the conformational stability of the PPII helix. In a series of well-defined model peptides Ac-(L-proline)$_9$-NH_2 (**1**), Ac-(Hyp)$_9$-NH_2 (**2**), and Ac-[Hyp(β-D-galactose)]$_9$-NH_2 (**3**) we demonstrate that contiguous *O*-glycosylation of Hyp residues causes a dramatic increase in the thermal stability of the PPII helix according to analysis of thermal melting curves. This represents the first quantitative data on the contributions of glycosylation to stabilizing the PPII conformation. Molecular modeling indicates the increase in conformational stability may be due to a regular network of interglycan and glycan−peptide hydrogen bonds, in which the carbohydrate residues form a hydrophilic "overcoat" of the PPII helix. Evidence of this shielding effect of the amide backbone may be provided by analysis of the circular dichroism bands, which indicates an increase in the ρ value of **3** relative to **1** and **2**. This study gives further insight into the effects of naturally occurring Hyp β-*O*-linked glycans on the PPII conformation as found in HRGPs in plant cell walls and also indicates that polyproline sequences may be suitable for the development of molecular scaffolds for the presentation of glycan structures.

Introduction

Once relatively obscure, the polyproline type II (PPII) conformation has become recognized for its presence in both folded and unfolded protein structures. It is characterized by having a left-handed helix ($\phi = -78°$ and $\psi = 146°$) with three amino acid residues per turn and *all-trans* amide bonds ($\omega = 180°$).[1] The PPII helix has now been implicated as a recognition domain in numerous protein−protein binding interactions,[2] which regulate diverse biological activities such as signal transduction, cell motility, and immune response.[3] The role of the PPII conformation in the protein-folding process has also come into focus, as there is mounting evidence that a proportion of unfolded protein structure preferentially adopts the PPII structure,[4] which has implications for the energetics of protein folding. However, the mechanism by which the PPII conformation is stabilized remains controversial.

Improved understanding of the characteristics of PPII structure has come from crystallographic,[1,5] spectroscopic,[6,7] and computational[8] analysis of model peptides. Both L-proline (Pro) and 4(*R*)-hydroxy-L-proline (Hyp) have demonstrated the highest propensity for forming the PPII conformation among the naturally occurring amino acids.[9] This is likely because their ϕ- and ψ-angles are ideally predisposed to do so; the ϕ-angle of Pro and Hyp is fixed at $-75°$ because the prolyl side chain is cyclized onto the polypeptide backbone. Furthermore, a ψ-angle of 150° leads to a favorable $n \rightarrow \pi^*$ interaction from the amide carbonyl oxygen atom (O_{i-1}) to the amide carbonyl group ($C'_i{=}O_i$).[10] Therefore, Pro and Hyp-rich domains of polypeptides bestow the extended PPII conformation with considerable structural stability.

(1) Cowan, P. M.; McGavin, S. *Nature* **1955**, *176*, 501–503.
(2) (a) Jardetzky, T. S.; Brown, J. H.; Gorga, J. C.; Stern, L. J.; Urban, R. G.; Strominger, J. L.; Wiley, D. C *Proc. Natl. Acad. Sci. U.S.A.* **1996**, *93*, 734–738. (b) Srinivasan, M.; Lu, D.; Eri, R.; Brand, D. D.; Haque, A.; Blum, J. S. *J. Biol. Chem.* **2005**, *280*, 10149–10155. (c) Rath, A.; Davidson, A. R.; Deber, C. M. *Biopolymers* **2005**, *80*, 179–185.
(3) (a) Kay, B. K.; Williamson, M. P.; Sudol, M *FASEB J.* **2000**, *14*, 231–241. (b) Mayer, B. J. *J. Cell Sci.* **2001**, *114*, 1253–1263. (c) Pawson, T. *Nature* **1995**, *373*, 573–580.
(4) (a) Adzhubei, A. A.; Sternberg, M. J. E. *J. Mol. Biol.* **1993**, *229*, 472–493. (b) Hamburger, J. B.; Ferreon, J. C.; Whitten, S. T.; Hilser, V. J. *Biochemistry* **2004**, *43*, 9790–9799. (c) Whittington, S. J.; Chellgren, B. W.; Hermann, V. M.; Creamer, T. P. *Biochemistry* **2005**, *44*, 6269–6275.
(5) (a) Saskisekharan, V. *Acta Crystallogr.* **1959**, *12*, 903–909. (b) Cartier, L.; Lotz, B *Macromolecules* **1998**, *31*, 3049–3054.
(6) (a) Steinberg, I. Z.; Harrington, W. F.; Berger, A.; Sela, M.; Katchalski, E. *J. Am. Chem. Soc.* **1960**, *82*, 5263–5279. (b) Isemura, T.; Okabayashi, H.; Sakakibara, S. *Biopolymers* **1968**, *6*, 307–321. (c) Okabayashi, H.; Isemura, T.; Sakakibara, S. *Biopolymers* **1968**, *6*, 323–330. (d) Grathwohl, C.; Wuthrich, K. *Biopolymers* **1981**, *20*, 2623–2633. (e) Lam, S. L.; Hsu, V. L. *Biopolymers* **2003**, *69*, 270–281.
(7) Helbecque, N.; Loucheux-Lefebvre, M. H. *Int. J. Pept. Prot. Res* **1982**, *19*, 94–101.
(8) (a) Tanaka, S.; Scheraga, H. A. *Macromolecules* **1974**, *7*, 698–705. (b) Bour, P.; Kubelka, J.; Keiderling, T. A. *Biopolymers* **2002**, *65*, 45–59.
(9) (a) Kelly, M. A.; Chellgren, B. W.; Rucker, A. L.; Troutman, J. M.; Fried, M. G.; Miller, A.-F.; Creamer, T. P. *Biochemistry* **2001**, *40*, 14376–14383. (b) Rucker, A. L.; Pager, C. T.; Campbell, M. N.; Qualls, J. E.; Creamer, T. P. *Proteins* **2003**, *53*, 68–75.
(10) Hinderaker, M. P.; Raines, R. T. *Protein Sci.* **2003**, *12*, 1188–1194.

10.1021/ja905724d

This aspect of the PPII conformation has inspired the development of molecular scaffolds that adopt predictable and well-defined conformations.[11] Proline-rich peptides that adopt a PPII conformation have the added advantages of being capable of crossing cell membranes[12] and being nonantigenic.[13] Therefore, these peptides have been used as molecular spacers,[14] molecular rulers,[15] cell-penetrating compounds,[12] and antibiotics.[12a,16]

Nature has also exploited the structural rigidity of the PPII conformation, as exemplified by its prevalence in both animal[17] and plant structural proteins. The hydroxyproline-rich glycoproteins (HRGPs) are widespread in the plant kingdom,[18,19] where they are associated with the plant cell wall and play important roles in plant growth, development, environmental sensing and signaling, and defense.[20] Consisting of several subclasses, HRGPs are characterized by a rigid PPII conformation formed by large amounts of Hyp that are extensively *O*-glycosylated, which is a unique post-translational modification of proteins.[18,19] The Hyp *O*-linked glycans are generally characterized by β-glycosidic linkages to either L-arabinose or D-galactose. Depending on the HRGP subclass, the glycan moiety may be a mono-, oligo-, or polysaccharide. The structural and functional consequences of glycosylation on HRGPs remains unclear, but efforts have been made to understand this modification. It has been suggested that the glycans increase HRGP solubility,[18] resistance to proteolytic degradation,[18] and thermal stability;[21] however, the extent of this stabilization has never been quantified or studied in well-defined model peptides.

Recent work by our group found that Hyp *O*-galactosylation in model diamides does not affect the stability of the *trans* amide bond as determined by measurement of the *trans*/*cis* amide equilibrium ($K_{trans/cis}$) or the prolyl C^{γ}-exo pucker, but close contacts between distant positions of the prolyl side chain and the galactose ring indicated that the glycan may affect the conformational stability of longer peptides.[22]

In an effort to understand the effects of Hyp *O*-glycosylation on the conformational stability of the PPII conformation, we report here on the synthesis and characterization of *O*-glycosylated polyproline model peptides. We were interested in providing quantitative data on any changes in conformational stability brought about by Hyp *O*-glycosylation and investigating the basis for these changes. We found that *O*-glycosylation of Hyp residues causes a dramatic increase in the thermal stability of the PPII helix according to analysis of thermal melting curves, which may be explained by a network of interglycan and glycan−peptide hydrogen bonds as determined by molecular-modeling experiments.

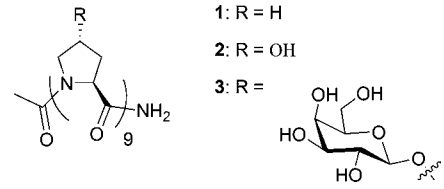

Figure 1. Model polyproline peptides **1**−**3**.

Scheme 1. Synthesis of Fmoc-[Hyp(β-D-Gal)]-OH (**4**)

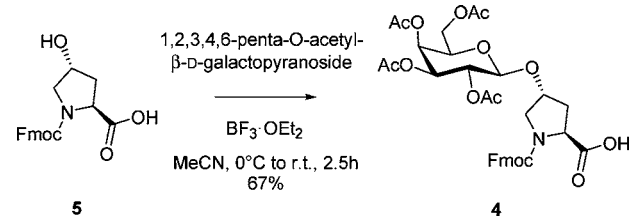

Results and Discussion

Synthesis of the Model Peptides 1−3. We constructed the following model polyproline homooligomers: Ac-$(Pro)_9$-NH_2 (**1**), Ac-$(Hyp)_9$-NH_2 (**2**), and Ac-[Hyp(β-D-Gal)]$_9$-NH_2 (**3**) (Figure 1).

The peptides **1** and **2** were synthesized as reference peptides to compare the effects of glycosylation on the structural stability of the PPII helix. D-Galactose residues were β-*O*-linked to Hyp, as this is the naturally occurring linkage as found in HRGPs. Contiguous *O*-glycosylation of the Hyp residues allows for maximum overlap of the sugar residues; with three residues per turn in the PPII helix, every fourth sugar residue is stacked on top of one another.[1,5−8] The *N*- and *C*-termini were amidated to prevent interference from charged groups, which can affect the stability of the PPII helix.[23]

The model peptides **1**−**3** were synthesized by solid-phase synthesis using Fmoc-protected building blocks on a 30−100 μM scale. The Fmoc-[Hyp(β-D-Gal(OAc)$_4$)]-OH building block was synthesized on the basis of the procedure of Arsequell, Sàrries, and Valencia using the Lewis acid $BF_3 \cdot OEt_2$ to promote the addition of 1,2,3,4,6-penta-*O*-acetyl-β-D-galactopyranoside[24] to commercially available Fmoc-Hyp-OH, which gives only the β-anomer in 67% yield (Scheme 1).[25] The assignment of the β-anomer was confirmed by the $^3J_{H1,H2}$ coupling constant of 8.0 Hz.

Circular Dichroism. Analysis of the far-ultraviolet circular dichroism (CD) spectra of **1**−**3** in water at 25 °C shows that all of the peptides exhibit positive maxima between 220 and

(11) Zhang, R.; Brownewell, F. E.; Madalengoitia, J. S. *J. Am. Chem. Soc.* **1998**, *120*, 3894–3902.
(12) (a) Sadler, K.; Eom, K. D.; Yang, J.-L.; Dimitrova, Y.; Tam, J. P. *Biochemistry* **2002**, *41*, 14150–14157. (b) Fernández-Carneado, J.; Kogan, M. J.; Pujals, S.; Giralt, E. *Biopolymers* **2004**, *76*, 196–203. (c) Fernández-Carneado, J.; Kogan, M. J.; Castel, S.; Giralt, E. *Angew. Chem., Int. Ed.* **2004**, *43*, 1811–1814. (d) Fillon, Y. A.; Anderson, J. P.; Chmielewski, J. *J. Am. Chem. Soc.* **2005**, *127*, 11798–11803. (e) Farrera-Sinfreu, J.; Giralt, E.; Castel, S.; Albericio, F.; Royo, M. *J. Am. Chem. Soc.* **2005**, *127*, 9459–9468. (f) Geisler, I.; Chmielewski, J. *Bioorg. Med. Chem. Lett.* **2007**, *17*, 2765–2768.
(13) Jasin, H. E.; Glynn, L. E. *Immunology* **1965**, *8*, 260–269.
(14) (a) Ungar-Waron, H.; Gurari, D.; Hurwitz, E.; Sela, M *Eur. J. Immunol.* **1973**, *3*, 201–205. (b) Maryanski, J. L.; Verdini, A. S.; Weber, P. C.; Salemme, F. R.; Corradin, G *Cell* **1990**, *60*, 63–72.
(15) (a) Stryer, L.; Haugland, R. P *Proc. Natl. Acad. Sci. U.S.A.* **1967**, *58*, 719–726. (b) Arora, P. S.; Ansari, A. Z.; Best, T. P.; Ptashne, M.; Dervan, P. B. *J. Am. Chem. Soc.* **2002**, *124*, 13067–13071.
(16) Otvos Jr, L. *Cell. Mol. Life Sci.* **2002**, *59*, 1138–1150.
(17) Nimni, M. E. *Collagen*; CRC Press: Boca Raton, FL, 1988.
(18) Lamport, D. T. A. *Nature* **1967**, *216*, 1322–1324.
(19) Sommer-Knudsn, J.; Bacic, A.; Clarke, A. E. *Phytochemistry* **1998**, *47*, 483–497.
(20) José, M.; Puigdom·enech, P. *New Phytol.* **1993**, *125*, 259–282.
(21) (a) Homer, R. B.; Roberts, K. *Planta* **1979**, *146*, 217–222. (b) Lamport, D. T. A., *Structure and Function of Plant Glycoproteins in The Biochemistry of Plants*; Academic Press: New York, 1980; Vol. 3, pp 501−540. (c) Ferris, P. J.; Woessner, J. P.; Waffenschmidt, S.; Kilz, S.; Drees, J.; Goodenough, U. W. *Biochemistry* **2001**, *40*, 2978–2987.
(22) Owens, N. W.; Braun, C.; O'Neil, J. D.; Marat, K.; Schweizer, F. *J. Am. Chem. Soc.* **2007**, *129*, 11670–11671.
(23) Kuemin, M.; Schweizer, S.; Ochsenfeld, C.; Wennemers, H. *J. Am. Chem. Soc.* **2009**, *131*, 15474–15482.
(24) Erwig, E.; Koenigs, W. *Ber. Dtsch. Chem. Ges.* **1889**, *22*, 2207–2213.
(25) Arsequell, G.; Sàrries, N.; Valencia, G. *Tetrahedron Lett.* **1995**, *36*, 7323–7326.

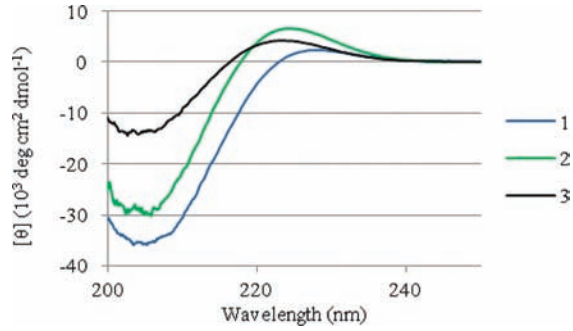

Figure 2. CD spectra of **1** (blue), **2** (green), and **3** (black) in water at 25 °C (0.4 mM).

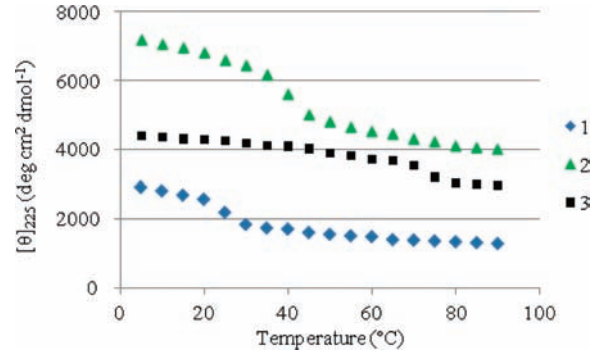

Figure 3. Ellipticity at 225 nm of **1** (diamonds), **2** (triangles), and **3** (squares) in water from 5 to 90 °C. Error limits for data points ranged from ±1−5%.

230 nm and negative maxima between 200 and 210 nm, which is characteristic of the PPII conformation (Figure 2).[26,27]

The peptide Ac-$(Hyp)_9$-NH_2 (**2**) showed a more intense positive band (λ_{max} at 225 nm, $[\theta] = 6600$ deg cm^2 dmol^{-1}) relative to Ac-$(Pro)_9$-NH_2 (**1**) (λ_{max} at 228 nm, $[\theta] = 2300$ deg cm^2 dmol^{-1}) but a weaker negative band (λ_{min} at 204 nm, $[\theta] = -31000$ and -37000 deg cm^2 dmol^{-1}, respectively), which is consistent with previous work.[28,29] The *O*-glycosylated model peptide Ac- [Hyp(β-D-Gal)]$_9$-NH_2 (**3**) also exhibited a stronger positive band (λ_{max} at 224 nm $= 4200$ deg cm^2 dmol^{-1}) relative to Ac-$(Pro)_9$-NH_2 (**1**) but a weaker negative band (λ_{min} at 204 nm, $[\theta] = -14{,}500$ deg cm^2 dmol^{-1}) relative to both **1** and **2**.

Overall, the CD spectra of Ac-[Hyp(β-D-Gal)]$_9$-NH_2 (**3**) relative to Ac-$(Hyp)_9$-NH_2 (**2**) shows a decrease in the relative intensity of both the positive and negative maxima (Figure 2), which may be attributed to a distortion of the PPII conformation.[30−33] Analysis of PPII model peptides by Kelly and coworkers has shown that incorporation of nonproline residues in polyproline peptides (from PPP to PAAP) leads to a similar decrease in the CD maxima from **3** to **2**.[9a] While this was correlated to a change in PPII conformation, the peptides were still considered to have significant PPII character. Overall, the molar ellipticities of **3** at λ_{max} and λ_{min} are consistent with naturally occurring HRGPs, such as GP1 (isolated from *Chlamydomonas reinhardtii*) and tomato extensin, which suggests that **3** adopts a similar PPII conformation to HRGPs.[21c]

Interpretation and rationalization of changes in CD spectra of the PPII conformation is not a straightforward process.[34] Horng and Raines found that when Hyp was replaced with 4(*R*)-fluoro-L-proline (Flp) in similar model polyproline peptides, a significant decrease in the intensity of the CD maxima was also observed.[29] Flp is known to stabilize the *trans* amide conformation and the C$^\gamma$-exo pucker, which would be expected to reinforce the PPII conformation, but instead caused an apparent decrease in PPII content based on the CD spectra. The authors gave no explanation for this apparent contradiction. Insight into the decrease in the intensity of the CD maxima of **3** may come from analysis of the relative band strength ρ[28] defined as the ratio of the maximum positive ellipticity to the maximum negative ellipticity. The ρ value for Ac-$(Pro)_9$-NH_2 and Ac-$(Hyp)_9$-NH_2 was found to be 0.06 and 0.21, which correlates well to previous studies of poly(Pro) (0.06) and poly(Hyp) (0.19).[28] In comparison, the ρ value for Ac-[Hyp(β-D-Gal)]$_9$-NH_2 was 0.29, which is higher than both **1** and **2**. An increase in ρ has been correlated to a distortion of the PPII conformation or decreased solvation of the peptide backbone carbonyl groups.[26] Therefore, it may be misleading to interpret the decrease in CD maxima from **3** to **2** as destabilization of the PPII conformation, as is typically done, and may reflect different factors, such as changes in hydration or shielding of the amide carbonyl groups.

Thermal Melting Experiments. To assess the conformational stability of the PPII helix, the CD spectra of **1**−**3** were monitored at 225 nm between 5 and 90 °C in pure water (Figure 3). Similar to other model peptides that exhibit PPII curves, there was a decrease in ellipticity at 225 nm as the temperature was increased.[7,35]

Plotting the CD curves of **1**−**3** as a function of temperature reveals an isodichroic point present for peptides **1**−**3** at 220, 215, and 211 nm, respectively (Figure 4), which is indicative of a coexistence of the PPII conformation with a higher temperature state.

The presence of both isodichroic points (Figure 4) and slight sigmoidal-type curves (Figure 3) is indicative that the polyproline peptides **1**−**3** undergo a conformational transition as the temperature is raised in aqueous solution. Previous studies have shown that based on the measurement of $^3J_{\alpha N}$ values of polyproline model peptides, while the PPII conformation is favored at low temperatures, it exists in equilibrium with the energetically similar[36] β-strand conformation ($\phi = -120°$ and $\psi = 120°$), which becomes more favored at high temperature.[35,37−42] The β-strand conformation is characterized by a

(26) Pysh, E. S. *Biopolymers* **1974**, *13*, 1563–1571.
(27) (a) Ronish, E. W.; Krimm, S. *Biopolymers* **1974**, *13*, 1635–1651. (b) Woody, R. W. *Adv. Biophys. Chem.* **1992**, *2*, 37–39.
(28) Brahmachari, S. K.; Bansal, M.; Ananthanarayanan, V. S.; Sasisekharan, V. *Macromolecules* **1979**, *12*, 23–28.
(29) Horng, J.-C.; Raines, R. T. *Protein Sci.* **2006**, *15*, 74–83.
(30) Ma, K.; Kan, L.-S; Kan, K; Wang, K. *Biochemistry* **2001**, *40*, 3427–3438.
(31) Rucker, A. L.; Creamer, T. P. *Protein Sci.* **2002**, *11*, 980–985.
(32) Kitamura, M.; Yamauchi, T.; Oka, M.; Hayashi, T. *Polym. Bull.* **2003**, *51*, 143–150.
(33) Vila, J. A.; Baldoni, H. A.; Ripoll, D. R.; Ghosh, A.; Scheraga, H. A *Biophys. J.* **2004**, *86*, 731–742.
(34) Woody, R. W. In *Circular Dichroism and the Conformational Analysis of Biomolecules*; Fasman, G. D., Ed.; Plenum Press: New York, 1996; p 56.
(35) Chen, K.; Liu, Z.; Kallenbach, N. R.; Baldwin, R. L. *Proc. Natl. Acad. Sci. U.S.A.* **2004**, *101*, 15352–15357.
(36) Dyson, H. J.; Wright, P. E. *Annu. Rev. Biophys. Chem.* **1991**, *20*, 519–538.
(37) Greenfield, N. J.; Fasman, G. D. *Biochemistry* **1969**, *8*, 4108–4116.
(38) Sreerama, N.; Woody, R. W. *Prot. Struct. Funct. Genet.* **1999**, *36*, 400–406.
(39) Shi, Z.; Olson, C. A.; Rose, G. D.; Baldwin, R. L.; Kallenbach, N. R *Proc. Natl. Acad. Sci. U.S.A.* **2002**, *99*, 9190–9195.
(40) Ding, L.; Chen, K.; Santini, P. A.; Shi, Z.; Kallenbach, N. R. *J. Am. Chem. Soc.* **2003**, *125*, 8092–8093.

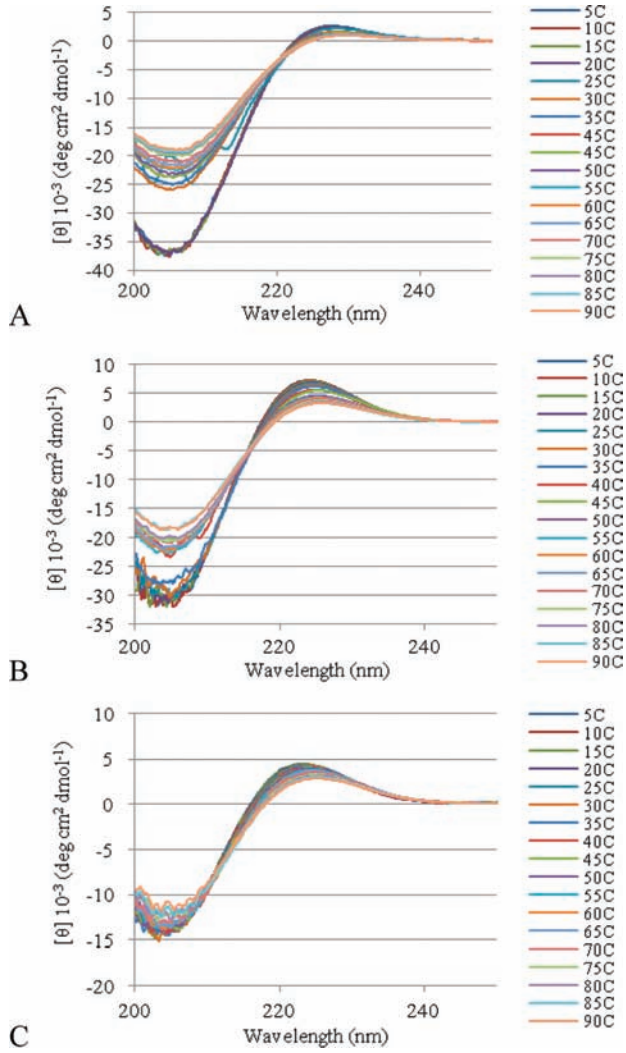

Figure 4. CD spectra of **1** (A), **2** (B), and **3** (C) from 5 to 90 °C in water from 200 to 250 nm. With increasing temperature, the intensity of both the positive and negative bands was found to decrease.

weak positive band near 220 nm and a negative band at 200 nm.[35,37−42] The higher temperature state is unlikely to be a random coil type conformation, which does not exhibit a net positive cotton effect.[43]

Here, the peptides **1**−**3** showed a distinctive transition based on the CD melting curves. The melting of the PPII helix has previously been attributed to a noncooperative transition, where destruction of the hydration shell leads to alteration or loosening of the PPII helix.[44] The sharpness of the transition seems to depend on the peptide sequence.[41] Model peptides incorporating nonproline residues alanine (Ala), glycine (Gly), and lysine (Lys) have exhibited both linear[9,35,39,42,45] and nonlinear[7,44,30,32,40] types of conformational transitions. A linear decrease in

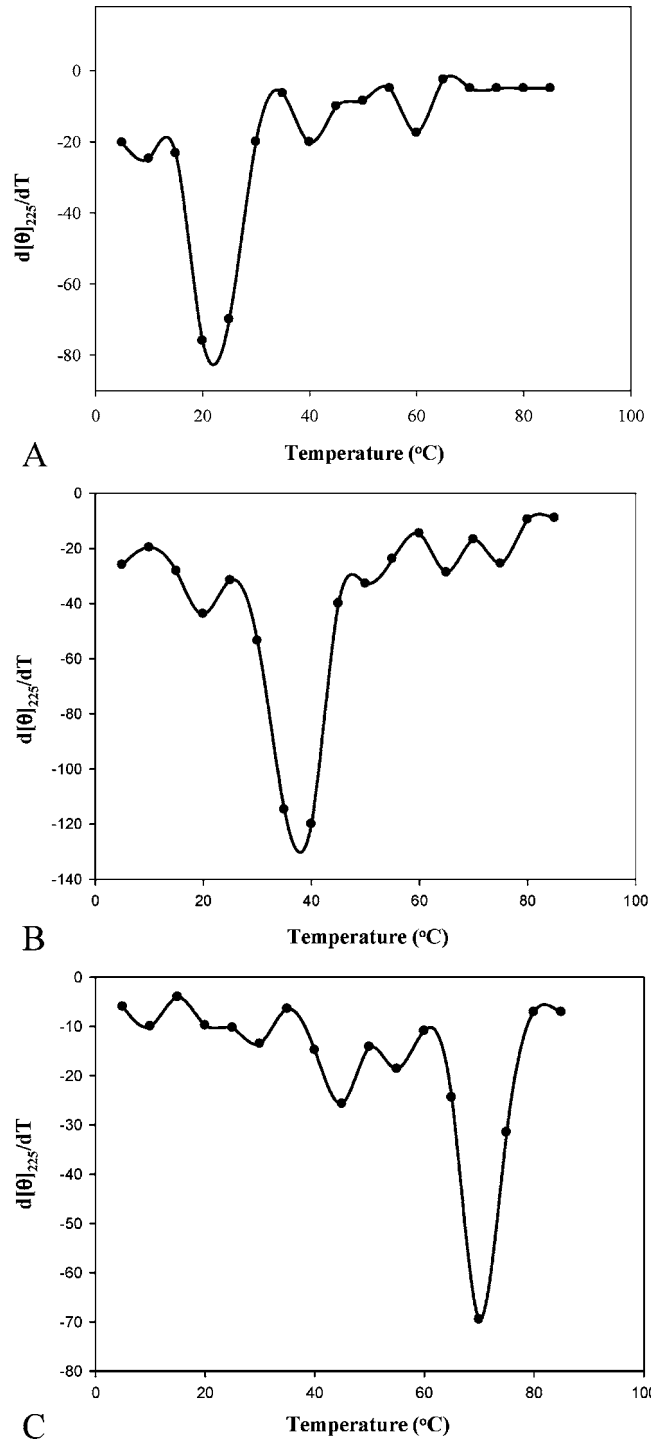

Figure 5. Spline curves of the first derivatives of the plot ellipticity as a function of temperature for **1** (A), **2** (B), and **3** (C).

ellipticity with no clear thermal transition has been attributed to similar polyproline peptides;[23,29] however, Horng and Raines have approximated melting temperature (T_m) values based on first-derivatives curves of the temperature-dependent CD spectra.[29] In an attempt to determine the T_m values of **1**−**3**, the first derivative of the melting curves was carried out as described by Horng and Raines (Figure 5).

The T_m for Ac-(Hyp)$_9$-NH$_2$ (T_m of 38 ± 3 °C) was found to be higher compared to Ac-(Pro)$_9$-NH$_2$ (T_m of 22 ± 3 °C), while the conformational transition occurred at a much higher temperature for Ac-[Hyp(β-D-Gal)]$_9$-NH$_2$ (T_m of 70 ± 3 °C). Nearly

(41) Avbelj, F.; Baldwin, R. L *Proc. Natl. Acad. Sci. U.S.A* **2003**, *100*, 5742–5747.
(42) (a) Eker, F.; Griebenow, K.; Schweitzer-Stenner, R. *J. Am. Chem. Soc.* **2003**, *125*, 8178–8185. (b) Eker, F.; Griebenow, K.; Cao, X.; Nafle, L. A.; Schweitzer-Stenner, R. *Proc. Natl. Acad. Sci. U.S.A.* **2004**, *101*, 10054–10059.
(43) Ronish, E. W.; Krimm, S. *Biopolymers* **1972**, *11*, 1919–1928.
(44) Makarov, A. A.; Adzhubei, I. A.; Protasevich, I. I.; Lobachov, V. M.; Esipova, N. G. *J. Prot. Chem.* **1993**, *12*, 85–91.
(45) (a) Drake, A. F.; Siligardi, G.; Gibbons, W. A. *Biophys. Chem.* **1988**, *31*, 143–146. (b) Kitamura, M.; Kakinoki, S.; Hirano, Y.; Oka, M. *Polym. Bull.* **2005**, *54*, 303–310.

identical melting points were calculated by fitting the data to a two-state transition model (Supporting Information). Therefore, it appears contiguous *O*-glycosylation of Hyp significantly stabilizes the PPII conformation.

While a complete understanding of the stabilization of the PPII helix has yet to be achieved, hydrogen-bonding interactions between the amino acids side chain to backbone nitrogen and carbonyl groups have been implicated.[4a,46] In model peptides, it has been found that after Pro and Hyp, glutamine (Gln), arginine (Arg), and lysine (Lys) are among the amino acids with the highest propensity to form PPII helices.[9b,46] This may explain the origin of the increase in thermal stabilization of Ac-[Hyp(β-D-Gal)]$_9$-NH_2 relative to Ac-(Hyp)$_9$-NH_2; the multiple sugar groups may form stabilizing hydrogen bonds to the peptide backbone in the PPII conformation, leading to considerable conformational stability. Hydration has also been proposed to contribute to the stability of the PPII conformation.[35,47] Therefore, the increase in stabilization upon contiguous *O*-glycosylation in Ac-[Hyp(β-D-Gal)]$_9$-NH_2 relative to Ac-(Hyp)$_9$-NH_2 may also be due to the change in solvation.

Previous work has shown that Hyp *O*-glycosylation does not lead to a measurable increase in the *trans*-prolyl amide population,[22] and as a result, it is unlikely that stereoelectronic effects can explain the increased stability of **3**. This is in contrast to homooligomers of 4(*R*)-fluoro-[29] and 4(*R*)-azidoproline[48] where stereoelectronic effects govern the increased stability of the PPII conformation.

Molecular Modeling. In order to gain further insight into the increase in thermal stability, a model of peptide **3** was subjected to energy minimization using the GROMOS force field. The results indicate that the galactose residues form a "hydrophilic overcoat" that spans the PPII helix. Hydrogen bonds are formed from the sugar hydroxyl groups ($C_{3(Gal)}$-OH_i) to the peptide backbone ($C{=}O_{i-2}$) and between galactose residues (*i* to *i*+1) (Figure 6); these may account for the large increase in conformational stability. Identical hydrogen bonds are seen for the α-galactosylated peptide segment suggesting that the nature of the glycosidic linkage is not crucial for the PPII stability (Supporting Information). A comparison of both modifications revealed only slight changes in interatomic distances, suggesting comparable stabilization effects.

Along with restricting the conformational freedom of peptides and proteins,[49] glycosylation is known to affect the solvation of peptides and proteins.[50] The proposed molecular model in Figure 6 indicates that the hydrophobic α-face of galactose shields the hydrophobic prolyl side chains from water, thereby potentially decreasing solvation of the peptide carbonyls; this is supported by relative changes in the band strength ρ in the CD spectra of **3** versus **2**. This also indicates that glycosylation may stabilize the PPII conformation through the formation of hydrogen bonding interactions, as well as through changes in the solvation of the PPII helix.

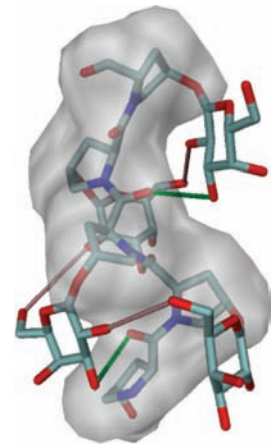

Figure 6. Molecular modeling of truncated **3** shows the surface area of the PPII backbone (shaded) with the D-galactose residues lying in the grooves of the PPII helix. Also shown are interglycan H-bonds ($C6(OH)_i$---$(OH)C2_{i+1}$) (pink) and glycan−peptide carbonyl backbone H-bonds ($C3$-$(OH)_i$---OC_{i-2}) (green). Modeling was performed using a polyproline II model helix and the GROMOS force field with the 53A6 parameter set for MD simulation.

Conclusions

In summary, analysis of the β-*O*-glycosylated polyproline model peptides indicates that Hyp *O*-galactosylation leads to a significant increase in conformational stability. A decrease in the intensity of CD maxima of **3** relative to **2** may be due to a distortion of the PPII conformation, decrease in PPII population, or shielding of the amide carbonyls by the hydrophobic α-galactose face. Molecular modeling suggests that the stabilization of **3** is likely due to multiple interglycan and glycan−peptide backbone hydrogen-bonding interactions. Since contiguous *O*-glycosylation leads to an increase in conformational stability, similar increases in the conformational stability of HRGPs likely also occur. Therefore, this study supports Lamport's hypothesis[21b] that naturally occurring β-linked glycans attached to oligoHyp peptide motifs stabilize the PPII conformation of HRGPs in plant cell walls. Whether noncontiguous glycosylation or other glycan structures affect this stability remains to be explored. Finally, our results suggest that PPII-based peptides provide a novel secondary structure scaffold to study carbohydrate-mediated interactions.[51]

Experimental Section

Materials and Methods. Protected amino acids were purchased from Bachem (King of Prussia, PA). Reagent-grade solvents were used without further purification. Thin-layer chromatography was performed on Si250F precoated glass plates of silica gel (250 μm). Column chromatography was performed on SilicaFlash P60 silica gel (40−63 μm).

Automated peptide synthesis was carried out using an Argonaut Quest 210 peptide synthesizer (San Carlos, CA) in 5 mL reaction vessels.

NMR spectra were obtained using a Bruker AMX-500 NMR spectrometer equipped with a triple resonance (^1H, ^{13}C, ^{15}N) gradient inverse probehead. Spectra were assigned based on 2D COSY and

(46) Stapley, B. J.; Creamer, T. P. *Protein Sci.* **1999**, *8*, 587–595.
(47) (a) Chen, K.; Liu, Z.; Zhou, C.; Shi, Z.; Kallenbach, N. R. *J. Am. Chem. Soc.* **2005**, *127*, 10146–10147. (b) Tiffany, M. L.; Krimm, S. *Biopolymers* **1968**, *6*, 1767–1770. (c) Pettitt, B. M.; Karplus, M. *Chem. Phys. Lett.* **1985**, *121*, 194–201. (d) Han, W.-G.; Jalkanen, K. J.; Elstner, M.; Suhai, S. *J. Phys. Chem. B* **1998**, *102*, 2587–2602. (e) Mezei, M.; Fleming, P. J.; Srinivasan, R.; Rose, G. D. *Proteins* **2004**, *55*, 502–507.
(48) Kümin, M.; Sonntag, L.-S.; Wennemers, H. *J. Am. Chem. Soc.* **2007**, *129*, 466–467.
(49) (a) Varki, A. *Glycobiology* **1993**, *3*, 97–130. (b) Dwek, R. A. *Chem. Rev.* **1996**, *96*, 683–720.
(50) Imperiali, B. *Acc. Chem. Res.* **1997**, *30*, 452–459.
(51) (a) Simpson, G. L.; Gordon, A. H.; Lindsay, D. M.; Promsawan, N.; Crump, M. P.; Mulholland, K.; Hayter, B. R.; Gallagher, T. *J. Am. Chem. Soc.* **2006**, *128*, 10638–10639. (b) Norgren, A. S.; Arvidsson, P. I. *J. Org. Chem.* **2008**, *73*, 5272–5278.

HSQC experiments. For ^{1}H NMR, minor isomers are listed between square brackets or as H′. A Waters Micromass ZQ 4000 mass spectrometer was used for electrospray ionization (ESI) mass spectrometry measurements.

Matrix-assisted laser desorption ionization (MALDI) data were acquired using a prototype quadrupole−quadrupole-TOF (QqTOF) mass spectrometer with photon pulses from a 20-Hz nitrogen laser (VCL 337ND, Spectra-Physics, Mountain View, CA) with 300 mJ energy/pulse. The sample solution (∼0.5 μL) was loaded onto a stainless steel target with the same volume of the saturated matrix solution (DHB in 1:1 (*v*/*v*) acetonitrile−water) and allowed to air dry.

CD measurements were carried out using a JASCO J-810 spectopolarimeter (Easton, MD) equipped with a Peltier thermoelectric temperature control system.

Peptide Synthesis and Purification. Peptide couplings were carried out using Fmoc-Rink Amide MBHA resin, which was initially allowed to swell in DCM for 1 h, and then was washed with DMF (5×). *Fmoc deprotections:* Deprotection of the Fmoc group was carried out using piperidine/DMF (1:4) (2 × 15 min), followed by a washing step with DMF (3×), DCM (3×), and again DMF (3×). *Peptide coupling:* Amino acids (Fmoc-Xaa-OH) (3 equiv) were coupled after preactivation (3 min) in DMF (4 mL) along with TBTU (4 equiv) and DIPEA (8 equiv). After mixing for 2.5 h, the resin was washed with DMF (3×), DCM (3×), and again DMF (3×). Coupling and deprotection reactions were monitored qualitatively by the Chloranil test.[52] *Capping:* After coupling of the first amino acid, the resin was capped using acetic anhydride/pyridine (1:9) (2 × 15 min), followed by a washing step with DMF (3×), DCM (3×), and DMF (3×). The same procedure was used to cap the *N*-terminus of the peptide. *Cleavage:* After a washing step of MeOH (3×) and DCM (6×), the peptides were cleaved from the resin by adding TFA/triisopropylsilane/water (18:1:1) (v/v/v) and mixing for 2 h. The resin was washed with TFA (2 × 5 mL) and DCM (2 × 5 mL) before concentration by codistillation with toluene (3 × 10 mL). *Acetate deprotection:* The sugar *O*-acetate groups were removed using methanol/hydrazine hydrate (6:1) (v/v) (2 × 3 h).[53] This deprotection step was carried out after the peptide was cleaved from the resin in order to limit acid-catalyzed deglycosylation of the β-linked sugars and to facilitate purification.

Semipreparative HPLC was performed on a Waters HPLC system (Milford, MA) using a Vydac C_{18} 5 μm particle size (10 mm × 250 mm) column (W. R. Grace & Co., Deerfield, IL). Analytical HPLC was carried out using an Atlantis C_{18} 5 μm particle size (4.6 mm × 150 mm) column (Waters Corp., Milford, MA). Detection of the products was achieved using a photodiode array monitoring at $\lambda = 210$ nm. Preparative HPLC was carried out using a gradient of 0−40% acetonitrile in water (0.1% TFA) over 30 min at a flow rate of 1 mL min^{-1}. Analytical HPLC was carried out using a gradient of 0−10% acetonitrile in water (0.1% TFA) over 30 min at a flow rate of 1 mL min^{-1}.

Ac-[Pro]$_9$-NH_2 (**1**) was synthesized using Fmoc-protected Rink amide MBHA resin on a 80 μM scale from Fmoc-L-Pro-OH. The synthesis was accomplished using the general procedure for peptide synthesis: analytical HPLC t_R 11.8 min; ^{1}H NMR (300 MHz, D_2O, 298 K) δ = 4.77−4.62 (m, 8H, Pro_α), [4.31−4.41, m, 1H, Pro_α], 3.73−3.92 (m, 8H, $Pro_{\delta1}$), 3.43−3.72 (m, 10H, $Pro_{\delta2}$, $Pro_{\delta1}'$), 2.19−2.47 (m, 9H, $Pro_{\beta1}$), 1.75−2.15 (m, 30H, $Pro_{\beta2}$, $Pro_{\gamma1,\gamma2}$, −COC*H*$_3$); HRMS (MALDI) calcd for $C_{47}H_{69}N_{10}O_{10}$ $(M + H)^+$ 933.5198, found $(M + H)^+$ 933.5226; HRMS (MALDI) calcd for $C_{47}H_{68}N_{10}NaO_{10}$ $(M + Na)^+$ 955.5022, found $(M + Na)^+$ 955.5041.

Ac-[Hyp]$_9$-NH_2 (**2**) was synthesized using Fmoc-protected Rink amide MBHA resin on a 100 μM scale from Fmoc-(2*S*,4*R*)-4-*O*-*tert*-butyl-Hyp-OH. The peptide cleavage step from the resin also removes the *O*-*tert*-butyl protecting groups: analytical HPLC t_R 9.1 min; ^{1}H NMR (500 MHz, D_2O, 298K) δ = 4.84−4.94 (m, 8H, Hyp_α), 4.57−4.70 (m, 9H, Hyp_γ), [4.49−4.56, m, 1H, Hyp_α], 3.86−4.00 (m, 8H, $Hyp_{\delta1}$), 3.63−3.86 (m, 10H, $Hyp_{\delta2}$, $Hyp_{\delta1}'$), 2.30−2.49 (m, 9H, $Hyp_{\beta1}$), 1.94−2.17 (m, 12H, $Hyp_{\beta2}$, −COC*H*$_3$); HRMS (MALDI) calcd for $C_{47}H_{69}N_{10}NaO_{19}$ $(M + Na)^+$ 1099.4563, found $(M + Na)^+$ 1099.4535.

Ac-[Hyp(β-D-Gal)]$_9$-NH_2 (**3**) was synthesized using Fmoc-protected Rink amide MBHA resin on a 30 μM scale from Fmoc-(2*S*,4*R*)-4-*O*-[2,3,4,6-tetra-*O*-acetyl-β-D-galactopyranose]-Hyp-OH (**4**). Because of the short elution time of the highly polar nonaglycosylated peptide, we purified the peptide before deacetylation at the protected Ac-[Hyp(β-D-Gal(OAc)$_4$]$_9$-NH_2 stage. This resulted in a much longer retention time on the analytical column (t_R 13.1 min) using a gradient of 25−100% acetonitrile in water over 30 min at a flow rate of 1 mL min^{-1} (Supporting Information). The single peak corresponded to a mass of 4070.31 Da consistent with the exact mass of $(M + Na)^+$. Deacetylation of Ac-[Hyp(β-D-Gal(OAc)$_4$]$_9$-NH_2 was achieved using methanol/hydrazine hydrate (6:1) (v/v) (2 × 3 h).[53] Excess hydrazine was removed under reduced pressure, and the deblocked glycopeptide **3** was purified from salts and acylated hydrazine by preparative reversed-phase HPLC using 100% water (t_R 5.7 min): analytical HPLC t_R 2.6 min; ^{1}H NMR (500 MHz, D_2O, 298K) δ = 4.84−4.96 (m, 8H, Hyp_α), [4.70−4.84, m, 1H, Hyp_α], [4.59−4.68, m, 2H, Hyp_γ], 4.45−4.58 (m, 16H, H_1, Hyp_γ), 4.07−4.22 (m, 9H, H_5), 3.60−4.00 (m, 54H, H_2, H_3, H_4, H_{6a}, H_{6b}, $Hyp_{\delta1}$), 3.44−3.59 (m, 9H, $Hyp_{\delta2}$), 2.50−2.67 (m, 9H, $Hyp_{\beta1}$), 1.95−2.16 (m, 12H, $Hyp_{\beta2}$, −COC*H*$_3$); HRMS (MALDI) calcd for $C_{101}H_{158}N_{10}NaO_{64}$ $(M + Na)^+$ 2557.9314, found $(M + Na)^+$ 2557.9208.

4-*O*-[(2,3,4,6-Tetra-*O*-acetyl)-β-D-galactopyranosyl]-N^α-fluoren-9-yl-methoxycarbonyl-(2*S*,4*R*)-4-hydroxyproline (4). This synthesis was based on the procedure of Arsequell, Sàrries, and Valencia.[25] Initially, 4-N^α-fluoren-9-ylmethoxycarbonyl-(2*S*,4*R*)-4-hydroxyproline (**5**) (2.00 g, 5.66 mmol, 1.0 equiv) was dissolved in dry acetonitrile (30 mL), cooled to 0 °C, and flushed with $Ar_{(g)}$. This was followed by the addition of 1,2,3,4,6-penta-*O*-acetyl-β-D-galactopyranoside (3.31 g, 8.49 mmol, 1.5 equiv) and $BF_3 \cdot OEt_2$ (2.13 mL, 16.9 mmol, 3.0 equiv). After being stirred for 30 min, the mixture was allowed to warm to ambient temperature and was stirred for an additional 2 h before being concentrated under reduced pressure. The resulting residue was suspended in water (30 mL), extracted into ethyl acetate (3 × 20 mL), and then dried (Na_2SO_4) and concentrated under reduced pressure. The product was purified by flash chromatography using first 10:10:1 DCM/EtOAc/MeOH then 4:4:1 DCM/EtOAc/MeOH to yield **4** as a clear oil (2.61 g, 3.81 mmol) (67.4%): $[\alpha]^{25}_D$ = −43.3 (*c* 1.1 CH_3OH); ^{1}H NMR (300 MHz, CD_3OD, 298K) δ = 7.73−7.87 (m, 2H, aromatic), 7.57−7.70 (m, 2H, aromatic), 7.25−7.47 (m, 4H, aromatic), 5.33−5.44 (broad dd, 1H, H_3), 5.03−5.21 (m, 2H, H_2, H_4), 4.71−4.81 (m, 1H, H_1, $J_{H1,H2}$ = 8.9 Hz), 4.01−4.55 (m, 8H, H_5, H_{6a}, H_{6b}, Hyp_α, Hyp_γ, −C(O)OCH_2C*H*, −C(O)OC*H*$_2$CH), 3.73−3.85 (m, 1H, $Hyp_{\delta1}$), 3.61−3.73 (m, 1H, $Hyp_{\delta2}$), 2.33−2.54 (m, 1H, $Hyp_{\beta1}$), 1.87−2.27 (m, 13H, $Hyp_{\beta2}$, −COC*H*$_3$); ^{13}C NMR (75 MHz, CD_3OD, 298K) δ = (173.8), (173.6), (173.4), (173.0), 172.0, 171.9, 171.5, 171.3, (156.6), 156.3, (145.8), 145.1, 142.6, (142.5), 129.1, (128.9), (128.5), 128.3, (126.4), 126.3, (121.1), 121.0, 102.0, (101.5), 79.6, (79.5), (72.2), 72.1, 70.33, (70.31), (68.97), 68.91, (68.6), 68.2, 63.0, (60.5), 60.4, (60.1), 59.3, (54.3), 53.9, 30.9, (30.1), (25.3), 23.9, 20.8, 20.7, 20.6, 20.3; HRMS (MALDI) calcd for $C_{34}H_{37}NNaO_{14}$ $(M + Na)^+$ 706.2112, found $(M + Na)^+$ 706.2147.

Circular Dichroism Spectroscopy. Purified samples of **1**−**3** were dried in vacuo for 24 h prior to weighing and then were dissolved in pure water at an approximate concentration of 0.4 mM and left to equilibrate for at least 24 h. The pH of the samples of **1**−**3** was determined at 25 °C after a two-point calibration (pH 4.0 and 10.0) to be 5.6, 6.5, and 6.1, respectively. Relative concentra-

(52) Vojkovsky, T. *Pept. Res.* **1995**, *8*, 236–237.
(53) Payne, R. J.; Ficht, S.; Tang, S.; Brik, A.; Yang, Y.-Y.; Case, D. A.; Wong, C.-H. *J. Am. Chem. Soc.* **2007**, *129*, 13527–13536.

tions were established by absorbance measurements at 214 nm.[54] The CD intensity and wavelength of the spectropolarimeter were calibrated using solutions of *d*-10-camphorsulfonic acid.[55] A blank spectrum of the solvent was subtracted, and for **3** the spectrum of methyl-β-D-galactopyranoside (3.6 mM) was subtracted (Supporting Information). For analysis, 300 μL of the sample was loaded in a rectangular quartz cell with a 0.1 cm path length. CD spectra were recorded using a scanning rate of 10 nm min^{-1}, response time of 4 s, data pitch of 0.1 nm, and bandwidth of 2 nm. For thermal melt experiments, a scan from 200 to 250 nm was performed at 5 °C intervals between 5 and 90 °C. Fluctuation in the temperature contributes an error value of ±1.0 °C to measurement of the temperature. The sample was allowed to equilibrate at each temperature for 10 min before the measurement was taken. The molar ellipticity per mean residue ([θ]) was calculated from the average spectrophotometer output (millidegrees) at 225 nm using the formula

$$[\theta] = (M\theta)/(10clr)$$

where M is the molecular weight of the sample (g·mol^{-1}), θ is the CD signal (millidegrees), c is the peptide concentration in g·L^{-1}, l is the path length of the cell (cm), and r is the number of amide bonds in the peptide (10). The reversibility of the thermal denaturation was judged by the recovery of the signal at the conclusion of the experiment (by 80−89%) at 25 °C. The temperature at the midpoint of the thermal transition (T_m) was estimated by calculating the first derivative of the molar ellipticity at 225 nm as a function of temperature. Values of T_m were estimated by the minimum of the spline curves of the corresponding data points using SigmaPlot software v11.0 (Systat Software, Inc.). Error in T_m can be assumed to be half the value of consecutive data points (±2.5 °C) along with the instrumental error (±0.5 °C).

The temperature at the midpoint of the thermal transition (T_m) was also determined by fitting ellipticity (mdeg) at 225 nm to a two-state model using Mathematica (v6.0) (Wolfram Research, Inc.) according to the equation

$$y = \frac{(\Delta N + \mathrm{mN}x) + (\exp[(\Delta H_m + x\Delta S_m)/(Rx)])(\Delta U + \mathrm{mU}x)}{1 + \exp(-[(\Delta H_m + x\Delta S_m)/(Rx)])}$$

where y is the optical parameter (mdeg), x is the temperature (kelvin), ΔH_m and ΔS_m are the differences between the folded and unfolded enthalpy and entropy at the transition midpoint (T_m), respectively, mN and mU are the slopes of the curve before and after the transition, respectively, and ΔN and ΔU are the zero temperature optical values of the low temperature state and the high temperature state, respectively. The value of T_m was calculated according to

$$T_m = \Delta H/\Delta S$$

The corresponding error value in T_m was calculated using the asymptotic standard error for ΔH and ΔS according to the equation

$$\sigma_T = [(\sigma_{\Delta H}{}^2/\Delta H^2) + (\sigma_{\Delta S}{}^2/\Delta S^2)]^{1/2}$$

where σ_T is the relative uncertainty in T_m, $\sigma_{\Delta H}$ is the uncertainty in ΔH, and $\sigma_{\Delta S}$ is uncertainty in ΔS. The calculated error in T_m (±0.2−0.5 °C) was less than the instrumental error.

Molecular Modeling. A truncated left-handed polyproline II (PPII) helix was generated with ϕ and Ψ-angles restricted to the characteristic regions of −78° and +146°, respectively.[1] The PPII helix has a perfect 3-fold rotational symmetry with a rise of approximately 3.1 Å per residue. Hydroxy functions and puckering geometries were introduced according to the ultrahigh resolution Hyp residue in the crystal structure of (Pro-Hyp-Gly)$_{10}$.[56] All five Hyp residues show "up" (C$^\gamma$-exo) puckering, with negative κ_1 angles varying between −22° and −27°.

The corresponding hydroxyproline PPII model peptide that was generated was the starting point for selective β-galactose and α-galactose configured substitutions of the Hyp residues. Individual D-galactose residues in $^4C_1$ conformations were separately introduced using the ATTACH function of the MAIN program package.[57] The initial structure of the peptide was generated using standard bond lengths, bond angles, and torsion angles.

The strain energy in the vicinity of each of the substitutions was generated in the GROMOS force field using the 53A6 parameter set optimized for molecular dynamics simulations.[57] For each substitution, the strain energy was subsequently minimized using the GROMACS package (version 3.3). This involved a brief steepest descents run that employed a maximum step size protocol of 1 Å and a maximum tolerance of 1000 kJ mol^{-1} nm^{-1}. This was followed by a more extensive conjugate gradients minimization with a tolerance of 100 kJ mol^{-1} nm^{-1}. Three-dimensional molecular representations were visualized with DINO version 0.9.1.[58]

Acknowledgment. We thank J. D. O'Neil for helpful discussions as well as the Natural Sciences and Engineering Research Council of Canada (NSERC), the Canada Foundation for Innovation (CFI), and the University of Manitoba for financial support.

Supporting Information Available: ^{1}H NMR spectra, analytical HPLC chromatograms, MALDI spectra of **1**−**4**, two-state transition plots, and molecular modeling figures.This material is available free of charge via the Internet at http://pubs.acs.org.

JA905724D

(54) Bretscher, L. E.; Jenkins, C. L.; Taylor, K. M.; Raines, R. T. *J. Am. Chem. Soc.* **2001**, *123*, 777–778.
(55) Wu, C. S.; Chen, G. C. *Anal. Biochem.* **1989**, *177*, 178–182.
(56) Okuyama, K.; Hongo, C.; Fukushima, R.; Wu, G.; Narita, H.; Noguchi, K.; Tanaka, Y.; Nishino, N. *Biopolymers* **2004**, *76*, 367–377.
(57) Oostenbrink, C.; Villa, A.; Mark, A. E.; Van Gunsteren, W. F. *J. Comput. Chem.* **2004**, *25*, 1656–1676.
(58) DINO: Visualizing Structural Biology (2002). http://www.dino3d.org.